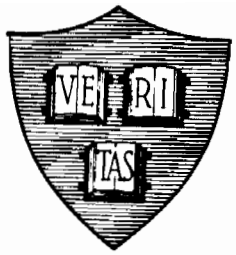

MECH-84

# INITIAL CRACK GROWTH TEARING RESISTANCE IN TRANSFORMATION TOUGHENED CERAMICS

J. W. Hutchinson

Division of Applied Sciences
HARVARD UNIVERSITY
Cambridge, Massachusetts 02138

June 1986

*To be published in a volume entitled*
***Advanced Materials for Severe Service Applications***
*by Elsevier Applied Science Publishers, edited by K. Iida*

# INITIAL CRACK GROWTH TEARING RESISTANCE IN TRANSFORMATION TOUGHENED CERAMICS

J. W. Hutchinson
Division of Applied Sciences
Harvard University
Cambridge, Massachusetts 02138

## Abstract

Transformation toughened ceramics display a resistance to crack advance requiring an increasing level of applied stress intensity to advance the crack tip. In this paper the initial slope of the resistance curve is determined. Two material models are considered. In each, only a net dilatational transformation is considered. In one, the transformation is assumed to be triggered at a critical value of the mean stress. In the other, the transformation is assumed to take place when the maximum shear stress reaches a crtical value.

## 1. INTRODUCTION

Tearing resistance in transformation toughened ceramics was predicted in [1] and [2] and R-curves have been experimentally measured in [3] for monoclinic zirconia containing a second phase of partially stabilized tetragonal zirconia. The high stresses at the tip of a macroscopic crack cause tetragonal particles of zirconia to transform to monoclinic form producing an irreversible transformation strain in the particles. Transformation of an unconstrained particle involves a dilatation of approximately 4% and a shear strain of about 16%. A particle embedded in an untransforming matrix transforms into a number of parallel twins with alternating signed shears so that the net shear in the particle is a small fraction of 16%. As discussed in [4], preliminary modeling which includes both shear and dilatational transformations indicates that the dilatational component is the more important in transformation toughening of ceramics. This will be the assumption made here. The dilatational transformation strain in the particle is denoted by $\theta_p^T$ and

the dilatational transformation strain of the matrix-particle combination is given by $\theta = c\theta_p^T$, where c is the volume concentration of the particles which is typical in the range from 20 to 40%.

Conditions for nucleation of the transformation in the matrix constrained particles are not well established [4]. Several candidates have been put forth and used in the various investigations of the mechanics of transformation toughening. Two of these will be used in this paper. The simplest from a mathematical point of view is the assumption that transformation will occur when the mean stress reaches a critical value, i.e. $\theta^T$ occurs in the particle-matrix combination when

$$\sigma_m \equiv \sigma_{kk} = \sigma_m^c \qquad \text{(Case A)} \tag{1}$$

The second is based on attaining a critical value of the maximum shear stress, i.e. $\theta^T$ occurs in the particle-matrix combination when

$$\tau_{max} = \tau_c \qquad \text{(Case B)} \tag{2}$$

This paper focusses on the behavior of a macroscopic crack immediately following initiation of crack growth. In particular, a theoretical calculation of the initial slope of the resistance curve is made for each of the two nucleation cases, A and B. the calculations are natural extensions of the work in [1], [2] and [4], and it is assumed that the reader is familiar with these papers. The present calculations invoke the following:

(I) All particles in a volume element transform, resulting in the full dilatational transformation $\theta^T$ when the critical stress condition, either A or B, is reached. In the nomenclature of [2], supercritical transformation is assumed.

(II) To determine the zone of transformation, the stress field at the tip of the crack without transformation will be used to locate the boundary where the critical stress condition is met. The perturbing influence of the transformation on the zone size and shape is ignored.

The limitations of these and other assumptions will be discussed at the end of the paper.

The analysis is carried out within the framework of plane strain. The transformation zone is assumed to be small compared to all in-plane geometric lengths so that small scale transformation

may be assumed. Thus, the field surrounding the transformation zone is the classical singular field for an elastic mode I crack of the form

$$\sigma_{ij} = \frac{K}{\sqrt{2\pi r}}\ \tilde{\sigma}_{ij}(\phi) \tag{3}$$

where K will be called the applied stress intensity factor and where r and $\phi$ are planar polar coordinates centered at the crack tip as indicated in Fig. 1. In particular, the distributions of the mean stress and the maximum shear stress are given by

$$\sigma_m = \frac{K(1+\nu)}{3}\left(\frac{\pi r}{2}\right)^{-1/2}\cos(\phi/2) \tag{4}$$

and

$$\tau_{max} = K(8\pi r)^{-1/2}\sin\phi \tag{5}$$

where $\nu$ is Poisson's ratio.

A singularity of the form (3) exists at the tip of the crack within the transformation zone except that its amplitude, $K_{tip}$, is altered by the existence of the transformation itself. The solution to the small scale transformation problem supplies the relation between $K_{tip}$ and K, and it is this relation which is used to predict the effects of transformation on the crack growth behavior. In [1], [2] and [4] it is assumed that a constant, critical value of crack tip intensity, $K_{tip}^c$, is required to initiate and sustain crack growth, and this assumption will be invoked here. The main aim of this paper is the prediction of dK/da just after initiation of crack growth under the assumption that

$$K_{tip} = K_{tip}^c \tag{6}$$

is maintained. It will be argued at the end of the paper that the full resistance curve should be computed under assumptions which are less restrictive than (I) and (II) invoked above. Such calcualtions will almost certainly require reasonably heavy numerical work. The present results, which are simple and exact under the stated assumptions, bring out essential trends.

The main result needed to carry out the present analysis is that for the effect on $K_{tip}$ of spots of transformation. As in Fig. 1, suppose the material in the two symmetrically disposed cylinders undergoes an unconstrained transformation dilatation $\theta^T$. With dA denoting the element of area of each spot, the change in $K_{tip}$ due to the transformation in the two spots is [2]

$$dK_{tip} = \Gamma dA\ d^{-3/2} \cos\left(\frac{3}{2}\beta\right) \tag{7}$$

where

$$\Gamma = E\theta^T/[3(1-\nu)\sqrt{2\pi}] \tag{8}$$

and E is Young's modulus.

## 2. dK/da FOR CASE A

Assuming the mean stress is given by (4) and assuming that transformation occurs when (1) is met, the transformation zone associated with any history of crack advance is the union of all material points for which (1) is attained at any time in the history. For a stationary crack experiencing a monotonically increasing K the boundary of transformation zone is given by (see Fig. 2)

$$R(\phi) = C_A\left(\frac{K}{\sigma_m^c}\right)^2 \cos^2(\phi/2) \tag{9}$$

where

$$C_A = 2(1+\nu)^2/(9\pi) \tag{10}$$

From (7), the near-tip intensity factor is given by

$$K_{tip} = K + \int_A \Gamma r^{-3/2} \cos(3\phi/2) dA \tag{11}$$

The integral in (11) is taken over the area A of the transformation zone in the upper half plane. For Case A, this integral is exactly zero giving for the stationary crack $K_{tip} = K$. Thus, by (6), initiation of crack growth in Case A occurs when

$$K = K_c \equiv K_{tip}^c \tag{12}$$

Now consider a small (infinitesimal) increment of crack growth $\Delta a$ with K increased so as to maintain (6). That is, $\Delta a$ and $\Delta K$ must be such that $\Delta K_{tip} = 0$. Refer to Fig. 3 which shows the initial transformation zone and the region for which $\sigma_m \geq \sigma_m^c$ for the crack of length $a+\Delta a$ loaded at $K+\Delta K$. Since the transformed zone is the union of all points which have experienced a mean stress greater or equal to $\sigma_m^c$, it follows that $K_{tip}$ is given by (11) where A is the union of $A_1$

and $A_2$ in Fig. 3. Furthermore, the integral over $A_2$ in (11) is identically zero for Case A, as is readily verified. Thus, for the initial increment of crack growth we require

$$\Delta K_{tip} = \Delta K + \int_{A^*} \Gamma r^{-3/2} \cos(3\phi/2) dA = 0 \tag{13}$$

where $A^*$ that part of $A_1$ not contained in $A_2$, i.e. the cross-hatched region in Fig. 3.

With the tip of the crack of length a+Δa as origin for the planar polar coordinates,

$$\int_{A^*} r^{-3/2} \cos(3\phi/2) dA = \int_{\phi^*}^{\pi} d\phi \int_{R_2(\phi)}^{R_1(\phi)} r^{-1/2} \cos(3\phi/2) dr$$

$$= 2\int_{\phi^*}^{\pi} [R_1(\phi)^{1/2} - R_2(\phi)^{1/2}] \cos\tfrac{3}{2}\phi \, d\phi \tag{14}$$

By (9),

$$R_2(\phi) = C_A \left(\frac{K+\Delta K}{\sigma_m^c}\right)^2 \cos^2(\phi/2) \tag{15}$$

while a direct calculation for small Δa gives

$$R_1(\phi) = C_A \left(\frac{K}{\sigma_m^c}\right)^2 \cos^2(\phi/2) + g(\phi)\Delta a \tag{16}$$

where

$$g(\phi) = \sin\alpha / \sin(\phi - \alpha) \tag{17}$$

and

$$\tan\alpha = (R' \sin\phi + R\cos\phi)/(R'\cos\phi - R\sin\phi) \tag{18}$$

with $(\,)' \equiv d(\,)/d\phi$. The term $g(\phi)\Delta a$ simply represents the change in the radial coordinate due to a small shift of the origin to the tip at a+Δa.

For Case A, a direct reduction of (18) gives $\alpha = 3\phi/2 - \pi/2$ and (17) gives

$$g(\phi) = -\cos(3\phi/2)/\cos(\phi/2) \tag{19}$$

The angle $\phi^*$ satisfies $R_1(\phi^*) = R_2(\phi^*)$. Equating the expressions in (15) and (16), dividing by Δa, and taking the limit as $\Delta a \to 0$, one finds

$$\lambda \equiv 2C_A \frac{K_c}{(\sigma_m^c)^2} \frac{dK}{da} = -\frac{\cos(3\phi^*/2)}{\cos^3(\phi^*/2)} \tag{20}$$

Another direct calculation using (16) and (17) gives

$$R_1^{1/2} - R_2^{1/2} = \frac{1}{2C_A^{1/2}} \frac{\sigma_m^c}{K_c} \cos(\phi/2) \left[ - \frac{\cos(3\phi/2)}{\cos^3(\phi/2)} - \lambda \right] \Delta a \tag{21}$$

to lowest order in $\Delta a$. Lastly, (13) with (14) and (21) require

$$\lambda = \zeta \int_{\phi^*}^{\pi} [\cos(3\phi/2)(\cos(\phi/2))^{-3} + \lambda] \cos(\phi/2) \cos(3\phi/2) d\phi \tag{22}$$

where

$$\zeta = \frac{2}{9\pi} \left( \frac{1+\nu}{1-\nu} \right) \frac{E\theta^T}{\sigma_m^c} \tag{23}$$

Equations (20) and (22) provide the relation between the initial slope of the resistance curve, as measured by the nondimensional combination $\lambda$, to the nondimensional parameter $\zeta$. The integration in (22) must be performed numerically. the simplest way to generate the relation between $\lambda$ and $\zeta$ is to treat $\phi^*$ as an independent variable and evaluate $\lambda$ from (20) and $\zeta$ from (22); $\phi^*$ must be in the range $(\pi/3, \pi)$. The results will be presented in a different nondimensional form which may be more convenient for comparison with experiment. The half-height of the transformation zone *at initiation* is given by

$$H = \frac{\sqrt{3}(1+\nu)^2}{12\pi} \left( \frac{K_c}{\sigma_m^c} \right)^2 \tag{24}$$

By eliminating $K_c$ in favor of H, it is readily shown that

$$\frac{(1-\nu)\sqrt{H}}{E\theta^T} \frac{dK}{da} = \frac{1}{4(\sqrt{3}\pi)^{1/2}} \frac{\lambda}{\zeta} \tag{25}$$

and this relation has been used to generate the plot in Fig. 4.

Before turning to Case B, we relate the present calculation for the initial slope of the resistance curve to an earlier calculation by McMeeking and Evans [1] which was performed to indicate the character of the resistance curve of a transformation toughened material.

## 3. McMEEKING AND EVANS' CALCULATION OF $\Delta K_{tip}$ VERSUS $\Delta a$ FOR CASE A

From (7) it can be seen that transformed material lying behind the wedge specified by $|\phi| \le \pi/3$ reduces the near-tip stress intensity. Figure 5 shows the reduction in crack tip intensity $-\Delta K_{tip}$ as a function of finite amounts of crack advance $\Delta a$ when the crack is advanced with K held *constant*. Using (11), one can show that this result is obtained from

$$-\frac{(1-\nu)\Delta K_{tip}}{E\theta^T\sqrt{H}} = \frac{16}{9\sqrt{6\pi}}\,\text{Real}\left\{\int_{\pi/3}^{\pi}([z(\phi)-\Delta a/H]^{-1/2}-[z(\phi)]^{-1/2})\cos(\phi/2)\cos(3\phi/2)d\phi\right\} \tag{26}$$

where H is given by (24) with K replacing $K_c$ and

$$z(\phi) = \frac{8}{3\sqrt{3}}\cos^2(\phi/2)[\cos\phi + i\sin\phi]$$

with $i = \sqrt{-1}$. The curve in Fig. 5 is the result of McMeeking and Evans [1] which was also plotted in their Fig. 5. This curve is not a resistance curve since it is computed with K held fixed so that $K_{tip}$ diminishes as $\Delta a$ increases. Nevertheless, it does clearly reveal the source of tearing resistance.

The full curve of $-\Delta K_{tip}$ versus $\Delta a$ in Fig. 5 is also useful for present purposes in that it enables us to see how rapidly the curve departs from its initial slope. In the limit as $\Delta a \to 0$, (26) gives

$$-\frac{(1-\nu)\sqrt{H}}{E\theta^T}\frac{dK_{tip}}{da} = .9518 \tag{27}$$

and this initial slope is shown in Fig. 5. Note that the full curve departs from the initial slope after very small amounts of crack advance. Similarly, we should expect that the initial slope of the resistance curve determined in this paper governs behavior only for a very small amount of crack advance.

## 4. dK/da FOR CASE B

The calculation of the initial slope of the resistance curve for Case B with the transformation condition in (2) follows closely that of Case A so less detail need be given. The main difference between the two cases is that $K_{tip}$ and K are not equal for monotonic loading of the stationary crack in Case B, and this must be taken into account.

The zone boundary for the *stationary crack* (see sketch in Fig. 2, Case B) is given by

$$R(\phi) = \frac{1}{8\pi}\left(\frac{K}{\tau_c}\right)^2 \sin^2\phi \tag{28}$$

and, from (11), one can show by direct integration that

$$\begin{aligned} K_{tip} &= K - \frac{2}{15\pi}\,\frac{E\theta^T K}{(1-\nu)\tau_c} \\ &= K - \frac{8}{15\sqrt{2\pi}}\,\frac{E\theta^T}{(1-\nu)}\,\sqrt{H} \end{aligned} \tag{29}$$

where, now,

$$H = \frac{1}{8\pi}\left(\frac{K}{\tau_c}\right)^2 \tag{30}$$

(We mention in passing that the result for the *steady-state problem* where the boundary is given by (28) for $|\phi| \le \pi/2$ and by $R\sin\phi = \pm H$ for $|\phi| > \pi/2$ can also be obtained analytically as

$$\begin{aligned} K_{tip} &= K - \frac{4(1+\sqrt{2})}{15\sqrt{\pi}}\,\frac{E\theta^T\sqrt{H}}{(1-\nu)} \\ &= K - \frac{.3632\ E\theta^T\sqrt{H}}{(1-\nu)} \end{aligned} \tag{31}$$

An approximation to this result for Case B was obtained and discussed in [4].)

Imposition of the condition for crack advance (6) on (29) gives the value of K asociated with initiation of crack advance, i.e.

$$K = K_c \equiv K_{tip}^c\,[1-\mu]^{-1} \tag{32}$$

where

$$\mu = \frac{2}{15\pi}\,\frac{E\theta^T}{(1-\nu)\tau_c} \tag{33}$$

Note that $K_c$ becomes unbounded for $\mu \to 1$. The present analysis, which neglects the perturbing influence of the transformation on the zone shape, is only accurate for relatively small values of $\mu$, as will be discussed in more detail at the end of the paper. Nevertheless, there is an effect of transformation on initiation of growth from the stationary crack in Case B whose ramifications have not been fully considered.

The equation governing the first increment of growth in (13) is replaced by

$$\Delta K_{tip} = (1-\mu)\Delta K + \int_{A^*} \Gamma r^{-3/2} \cos(3\phi/2) dA = 0 \tag{34}$$

where $A^*$ is again defined in Fig. 3, except that now regions $A_1$ and $A_2$ are defined by the transformation condition (2). Equation (14) continues to hold where now

$$R_2(\phi) = \frac{1}{8\pi}\left(\frac{K+\Delta K}{\tau_c}\right)^2 \sin^2\phi \tag{35}$$

and

$$R_1(\phi) = \frac{1}{8\pi}\left(\frac{K}{\tau_c}\right)^2 \sin^2\phi + g(\phi)\,\Delta a \tag{36}$$

In addition, after some algebraic manipulation one finds that $g(\phi) = -3\cos\phi$. The angle $\phi^*$ for which $R_1(\phi^*) = R_2(\phi^*)$ satisfies

$$\lambda_B \equiv \frac{1}{4\pi}\frac{K_c}{\tau_c^2}\frac{dK}{da} = -\frac{3\cos\phi^*}{\sin^2\phi^*} \tag{37}$$

Finally, in the limit $\Delta a \to 0$, (34) gives

$$(1-\mu)\lambda_B = \tfrac{5}{4}\mu\int_{\phi^*}^{\pi} [3\cos\phi\,(\sin\phi)^{-2} + \lambda_B]\sin\phi\,\cos(\tfrac{3}{2}\phi)d\phi \tag{38}$$

Equations (37) and (38) provide the relation between $\lambda_B$ and the parameter $\mu$. With

$$H = \frac{1}{8\pi}\left(\frac{K_c}{\tau_c}\right)^2 \tag{39}$$

as the half-height of the zone at *initiation of growth*, one also finds

$$\frac{(1-\nu)\sqrt{H}}{E\theta^T}\frac{dK}{da} = \frac{4}{15\sqrt{2\pi}}\frac{\lambda_B}{\mu} \tag{40}$$

This is the equation used to plot the curve in Fig. 6. The curve becomes unbounded as $\mu \to 1$, but the results are not trustworthy at values of $\mu$ this large as already mentioned.

## 5. LIMITATIONS OF PRESENT ANALYSIS AND SUGGESTIONS FOR FURTHER WORK

As it becomes available, resistance curve data should supply valuable additional information to which the mechanics models can be compared and calibrated. The present calculations are just a first step in predicting resistance curves from the mechanics models. Hopefully, a comparison of theoretical predictions with experimental resistance curve data should shed further light on which, if either, of the two transformation conditions, A or B, is appropriate. Given either A or B as a starting point, there are three main limitations to the present results.

Firstly, as indicated by the example in Fig. 5, the initial slope of the resistance curve which has been computed here is expected to replicate the resistance curve for only small amounts of crack growth. For comparison with experimental data it is essential that the full resistance curves be calculated.

Secondly, the results in this paper, which were computed using the unperturbed stress field to locate the boundary of the transformation zone, are valid only for small $\zeta$ or $\mu$. Analyses which account for the perturbation of the zone were carried out in [2] and [5] for the steady-state, small scale transformation problem for Case A. Those analyses indicate that the results of the unperturbed analysis are accurate for values of $\zeta$ as large as about 1/2, and we expect the present results to be similarly limited. Comparable results for Case B do not exist. The unboundedness of $K_c$ and of the nondimensional parameter involving the initial slope of the resistance curve in Fig. 6 should also emerge from a full analysis of Case B, but the value of $\mu$ at which the unboundedness occurs will not necessarily be unity.

Lastly, there is increasing evidence [4] that supercritical transformation in which the material element undergoes complete transformation to $\theta^T$ may be the exception rather than the rule. Observations indicate that the density of transformed particles falls off smoothly, and not

abruptly, with distance from the crack tip. This suggests that models based on subcriticial transformation should also be analyzed.

## ACKNOWLEDGEMENT

This work was supported in part by the National Science Foundation under Grant MSM-84-16392, and by the Division of Applied Sciences, Harvard University. The author acknowledges helpful discussions with A. G. Evans and R. M. McMeeking.

## REFERENCES

(1) McMeeking, R. M. and Evans, A. G., J. Am. Ceram. Soc. **65**, 242-246 (1982).

(2) Budiansky, B., Hutchinson, J. W. and Lambropoulos, J. C., Int. J. Solids Structures **19**, 337-355 (1983).

(3) Swain, M. V. and Hannink, R. H. J., Advances in Ceramics (American Ceram.Soc.), Vol. 12, 225 (1984).

(4) Evans, A. G. and Cannon, R. M., Acta Metall. **34**, 761-800 (1986).

(5) Rose, L. R. F., "The Size of the Transformed Zone During Steady-State Cracking in Transformation-Toughened Materials", Aero. Research Report, Melbourne, Australia (1986).

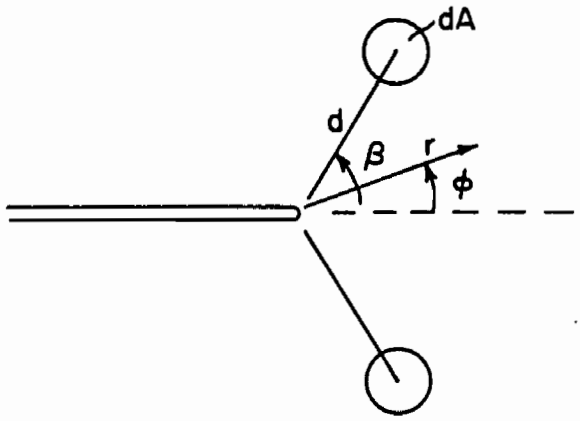


Fig. 1 Conventions at the crack tip.


Case A Case B

Fig. 2 Notation and sketches of boundary of transformation zones.

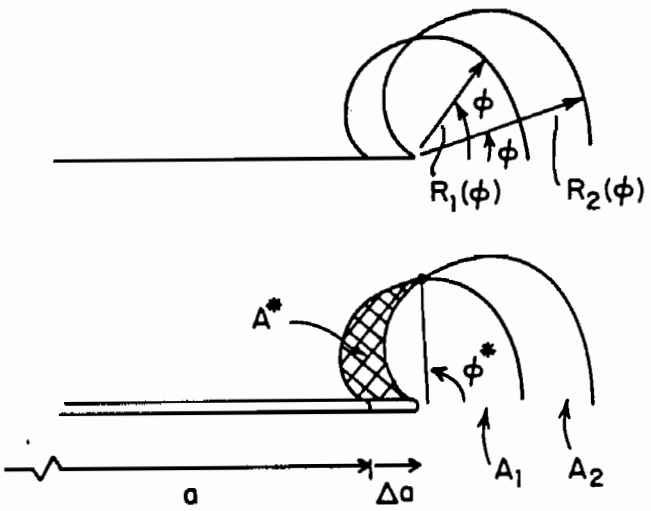


$A_1$: Transformation zone of initial stationary crack

$A_2$: Region for which $\sigma_m \geq \sigma_m^c$ for crack of length $a + \Delta a$ at $K + \Delta K$

Fig. 3 Zone of stationary crack at initiation of crack growth at K, and region for which mean stress exceeds $\sigma_m{}^c$ following crack advance $\Delta a$ with applied stress intensity increased to $K+\Delta K$. Sketches are for Case A with similar sketches for Case B.

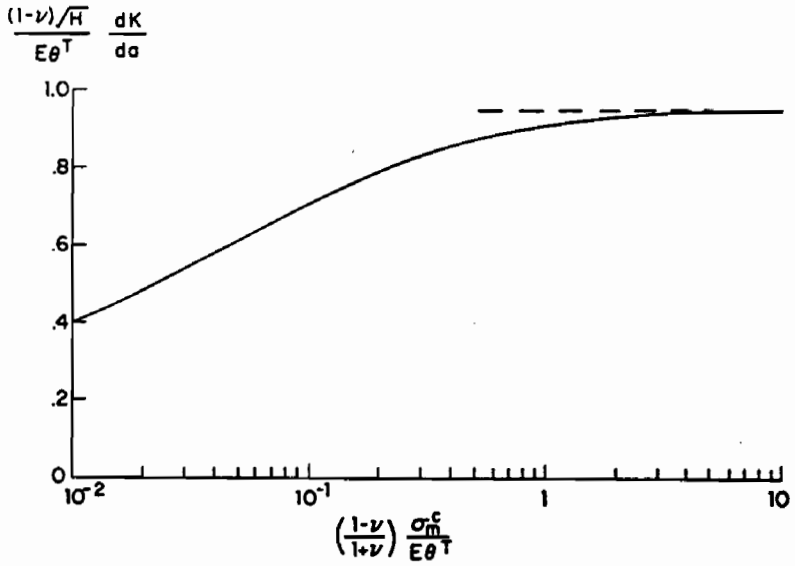


Fig. 4 Nondimensional initial slope of resistance curve for Case A where H is the transformation zone half-height at initiation of growth.

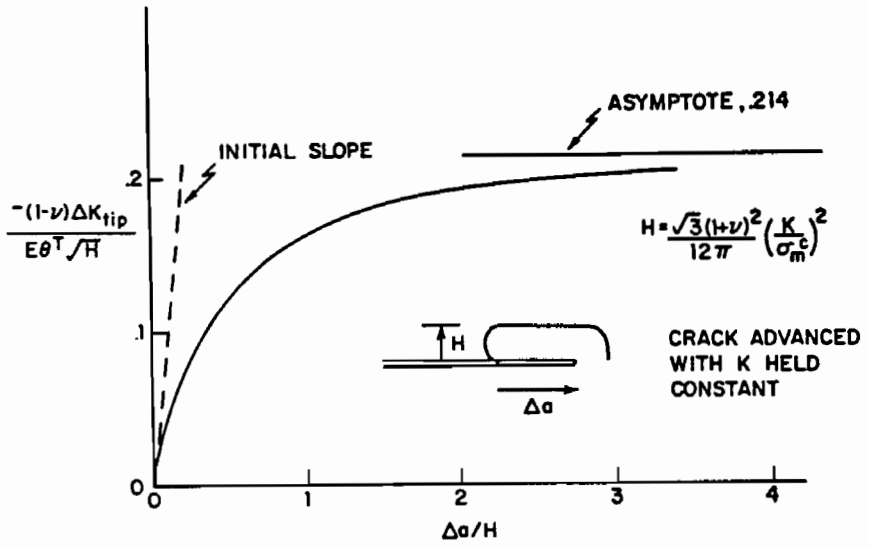


Fig. 5 Reduction in near-tip intensity as a function of crack advance when applied stress intensity factor is held constant [1].

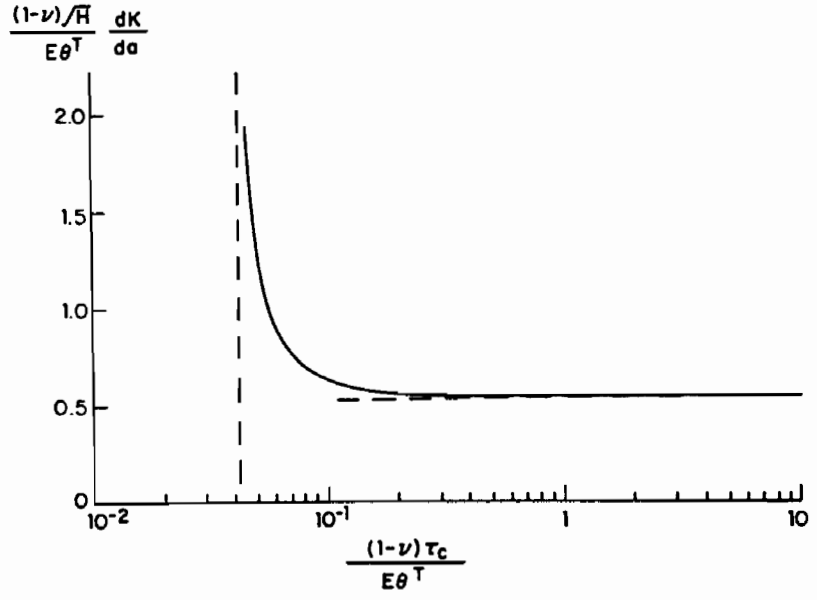


Fig. 6 Nondimensional initial slope of resistance curve for Case B where H is the transformation zone half-height at initiation of growth.